Journal of Magnetic Resonance 212 (2011) 1–10

Contents lists available at ScienceDirect

Journal of Magnetic Resonance

journal homepage: www.elsevier.com/locate/jmr

Perspectives in Magnetic Resonance

Dynamics of biomolecules from picoseconds to seconds at atomic resolution

Dennis A. Torchia *

Building 5, Room 128, NIH, Bethesda, MD 20892-0520, USA

ARTICLE INFO

Article history:
Received 21 June 2011
Available online 22 July 2011

Keywords:
Protein
Dynamics
Spectral density
Labeling
Spin
Order parameter
Relaxation
RDC
Dispersion
Exchange
TROSY

ABSTRACT

Although biomolecular dynamics has been investigated using NMR for at least 40 years, only in the past 20 years have internal motions been characterized at atomic resolution throughout proteins and nucleic acids. This development was made possible by multidimensional heteronuclear NMR approaches that provide near complete sequential signal assignments of uniformly labeled biomolecules. Recent methodological advances have enabled characterization of internal dynamics on timescales ranging from picoseconds to seconds, both in solution and in the solid state. The size, complexity and functional significance of biomolecules investigated by NMR continue to grow, as do the insights that have been obtained about function. In this article I review a number of recent advances that have made such studies possible, and provide a few examples of where NMR either by itself or in combination with other approaches has paved the way to a better understanding of the complex relationship between dynamics and biomolecular function. Finally, I discuss prospects for further advances in this field.

1. Introduction

Theoretical and experimental work directed at using NMR to study molecular dynamics in solution and solid states was initiated shortly after the first successful NMR experiments in bulk matter. By 1960, the basic theory underlying virtually all of the techniques used today to study biomolecular dynamics had been developed and verified by experiment [1]. The introduction of pulsed Fourier transform spectroscopy and superconducting magnets as well as improvements in instrumentation opened the way to the first atomic resolution studies of protein dynamics [2–6]. However, available methodology limited measurements to a few resolved and assigned signals. As a consequence of further improvements in instrumentation, the development of multidimensional NMR spectroscopy, and the introduction of methodology for labeling biomolecules uniformly or specifically with $^{2}H/^{13}C/^{15}N$, assignment of chemical shifts is straight-forward. Once signals are assigned, measurements can be made of relaxation rates, residual anisotropic interactions (dipolar, quadrupolar and chemical shift), relaxation dispersion (RD) profiles, magnetization- and hydrogen-exchange rates, yielding site-specific information about dynamics on timescales in the range of ps to s, as summarized in Fig. 1. In the past decade, the potential of NMR to provide information about dynamics with atomic resolution has been realized for increasingly more complex systems, in solids as well as in solution. In this article I present examples of recent methodological advances in which information on dynamics has provided insights about function. I also discuss the prospects of further advances in NMR methodology that together with other biophysical and biochemical approaches have the potential to provide further insights about the complex molecular mechanisms that underlie function.

2. Labeling of proteins and nucleic acids

Nearly all contemporary studies of protein dynamics are performed on protein samples that are produced by *Escherichia coli*. Proteins are labeled in a variety of ways. The most common among these are uniform labeling with ^{2}H, ^{13}C and/or ^{15}N and sparse labeling of methyl sites. The availability of such labeled samples has stimulated the development of a myriad of multidimensional heteronuclear NMR experiments that provide atomic resolution information about protein dynamics on a wide range of timescales.

While studies of protein dynamics have benefited greatly by available labeling procedures, interest in novel methods of protein expression and labeling remains high. It is important to have alternatives to *E. coli* expression systems: for example, eukaryotic-cell and cell-free expression systems, in order to obtain proteins that have posttranslational modifications, and to bypass cell toxicity problems, respectively. In addition, in order to relieve severe overlap of signals in spectra of large proteins, stereo-array (SAIL) labeling and segmental labeling approaches are being pursued. These

* Fax: +1 301 496 0825.
E-mail address: dtorchia@dir.nidcr.nih.gov

1090-7807/$ - see front matter © 2011 Elsevier Inc. All rights reserved.
doi:10.1016/j.jmr.2011.07.010

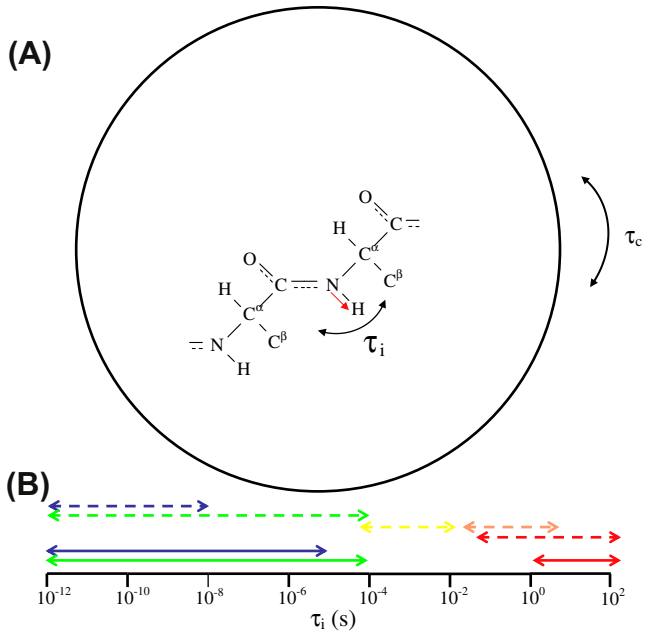

Fig. 1. (A) Schematic depiction of a small segment of a uniformly ^{15}N enriched polypeptide chain within a globular protein. For simplicity the protein is assumed to be a sphere whose rigid-body reorientation is characterized by a single correlation time τ_c. The reorientation of an N–H bond vector depends upon τ_c as well as on reorientation resulting from local motions described by internal correlation time (s), τ_i. Using a sample that is uniformly labeled with ^{15}N and/or ^{13}C, a variety of heteronuclear multidimensional NMR experiments are available that provide information about internal dynamics on a wide range of timescales at sites throughout the protein. In (B) the lengths of the colored solid (dashed) arrows depict the approximate range of timescales that are probed by various types of NMR measurements in solids (solution). Relaxation measurements provide information about fast internal dynamics on timescales indicated by the blue arrows. Measurements of residual dipolar couplings in solution, or powder patterns in solids, elucidate dynamics on timescales indicated by the green arrows. Relaxation dispersion profiles reveal slow conformational changes on timescales, shown by the yellow arrow, that modulate isotropic chemical shifts. Yet slower motions, orange arrow, are made manifest by magnetization exchange experiments. Slower motions still, red arrows, are revealed by measurements of hydrogen exchange.

and other novel methods for producing and labeling proteins are discussed in a recent overview of current developments in this field [7].

Labeled small oligomers of DNA and RNA are often prepared by chemical synthesis. More efficient and cost effective methods for preparing larger RNAs, labeled with $^{2}H/^{13}C/^{15}N$, using *in vitro* transcription were first developed in the early 1990s [8] opening the way for heteronuclear NMR measurements of RNA structure and dynamics. There is great current interest in developing new approaches to prepare labeled RNA [9], as the number of known functions carried out by RNA continues to grow. In addition, there has been significant recent progress in developing new reagents for binding paramagnetic metal ions, particularly lanthanides, at specific sites in proteins and nucleic acids [10].

3. Spin relaxation

Nearly all biomolecular relaxation studies have involved measurements of relaxation rates of ^{13}C, ^{15}N or ^{2}H spins. Dipole–dipole (DD) and chemical shift anisotropy (CSA) interactions are the dominant relaxation mechanisms for ^{13}C and ^{15}N, while the quadrupole interaction (Q) is responsible for ^{2}H relaxation. The general theory of spin relaxation was developed for these mechanisms in the 15 years following the invention of NMR, and described in a number of classic publications [1]. Nevertheless, another two decades passed before the practical impact of DD/DD [11] and DD/CSA [12] cross-correlation upon relaxation measurements was fully appreciated. With appropriate experimental design [13], relaxation is mono-exponential and relaxation rates can be analyzed using well known equations, all of which involve sums of products of interaction strengths, ω_λ, (λ = DD, CSA, Q) and spectral densities. For example, when overall reorientation is isotropic, R_1 is given by [13]

$$R_{1S} = (\omega_{DD}/2)^2[J_{DD}(\omega_I - \omega_S) + 3J_{DD}(\omega_S) + 6J_{DD}(\omega_I + \omega_S)] + (2/15)\omega_{CS}^2 J_{CS}(\omega_S)$$
$$R_{1D} = 3\omega_Q^2[J_Q(\omega_D) + 4J_Q(\omega_D)]$$

where $S = {}^{13}C$ or ^{15}N, is dipolar relaxed by spin I, $D = {}^{2}H$ and

$$\omega_{DD} = (\mu_o/4\pi)\gamma_I\gamma_S\hbar/r_{IS}^3, \omega_{CSA} = \omega_S\Delta\sigma\sqrt{1+\eta_{CSA}^2/3}, \omega_Q = (eqQ/4\hbar)\sqrt{1+\eta_Q^2/3} \quad (1)$$

The spectral densities, $J(\omega)$, which are a measure of the density of fluctuations at frequency ω, contain the information about dynamics. Clearly, relaxation data provide information about spectral densities only if values of ω_λ are known, and considerable effort has been made to measure these values in model compounds and in biopolymers in solid and solution states. Values of ω_λ and orientations of the corresponding interaction tensors have been obtained using (large) single crystals of model compounds [14,15]. Recently, values of the chemical shift anisotropy and asymmetry parameter, $\Delta\sigma$ and η_{CSA} respectively [15], have been measured [16–18] at backbone ^{15}N and ^{13}C sites throughout uniformly labeled proteins in (micro)crystalline and solution states. These studies have revealed the extent to which $\Delta\sigma$ and η_{CSA} are affected by variations in local chemical and molecular structure. A Herzfeld–Berger analysis of slow magic angle spinning (MAS) experiments has provided values of $\Delta\sigma$ and η_{CSA} in crystalline GB1 [16] that are in close agreement with results obtained for ubiquitin and GB3 in solution from residual dipolar coupling (RDC), residual chemical shift anisotropy (RCSA) and cross-correlated relaxation data [17,18]. As seen in Table 1, $\langle\Delta\sigma\rangle$ and $\langle\eta_{CSA}\rangle$ depend upon secondary structure for both $^{13}C'$ and ^{15}N spins. Large sequence-dependent variations in $\Delta\sigma$ (20–40 ppm) and η_{CSA} (0.2–1.0) have been observed in crystalline GB1 for C^α spins [19].

A joint analysis of $^{13}C'–^{1}H^N$ and $^{15}N^H–^{1}H^N$ RDC data, carefully measured for five independent alignments of GB3 [20] indicates

Table 1
Average values of backbone ^{15}N, $^{13}C'$ CSA magnitudes, $\langle\Delta\sigma\rangle$[a], and asymmetry parameters, $\langle\eta_{CSA}\rangle$, in proteins.

Protein	Spin	Method	$\langle\Delta\sigma\rangle$ α-helix	$\langle\Delta\sigma\rangle$ β-sheet	$\langle\Delta\sigma\rangle$ all sites	$\langle\eta_{CSA}\rangle$ α-helix	$\langle\eta_{CSA}\rangle$ β-sheet	$\langle\eta_{CSA}\rangle$ all sites
GB1	^{15}N	HB-sMAS[b]	173	159	164	0.2–0.3	0.2–0.3	0.2–0.3
GB3	^{15}N	RDC/RCSA	173	162	167	0.23	0.31	0.25
GB1	$^{13}C'$	HB-sMAS	−126	−117	−119	0.53	0.72	0.65
Ubiquitin[c]	$^{13}C'$	RDC/RCSA	−135	−121	−125	0.53	0.82	0.72

[a] In ppm. NB, the sign of the shift anisotropy is opposite that of the shielding anisotropy.
[b] Herzfeld–Berger slow MAS.
[c] The $\langle\Delta\sigma\rangle$ are 3% less than those published to compare with solid-state values [17].

that the N–H bond length is uniform throughout the protein to within ±0.5%. Analysis of RDC and RQC data has also shown that C^{α}–H, C^{methyl}–H distances [21,22] and C^{methyl}D quadrupole coupling constants [23] are uniform in proteins as well. Due to zero point averaging (of stretching and bending motions), N–H and C–H bond lengths obtained by NMR are 2–2.5% larger than average bond lengths obtained by calculation or by other types of physical measurements [20]. It is reasonable to suppose that zero point motions increase effective bond lengths by comparable amounts in nucleic acids as well, and this supposition is supported by experimental data [24].

Chemical shift tensors of ^{15}N and ^{13}C spins at various positions in nucleotide base and ribose sites in RNA and DNA have been determined from a combined analysis of RCSA data and dipole–dipole/CSA cross-correlated relaxation rates. The shift tensor components determined in the liquid state are in good agreement with predictions of quantum chemical calculations and solid-state measurements of CSA tensors in mononucleotides [24–27]. A thorough review of chemical shift measurements and their biological applications has been presented recently [15].

4. Measurements of relaxation rates

The first proton-detected 2D relaxation measurements of heteronuclei (^{13}C or ^{15}N) at sites throughout proteins in solution were carried out about 20 years ago [28,29]. Since that time, many refinements have been incorporated into the experiments to reduce systematic errors resulting from cross correlation, resonance offset, water saturation etc., so that experimental uncertainties are now typically a few percent. Although most relaxation studies of protein backbone dynamics have been carried out on ^{15}N labeled samples, because of the ease and low cost of sample preparation, complementary information about backbone motions has come from relaxation measurements of $^{13}C^{\alpha}$ and $^{13}C'$ labeled samples as well. Most studies of sidechain dynamics have been of methyl sites. Dipolar cross correlation, which causes multi-exponential relaxation of ^{13}C transverse magnetization of $^{13}CH_3$ moieties, is difficult to fully suppress. This problem has been circumvented by measuring ^{2}H [30,31] and ^{13}C [32] relaxation in $^{13}C^{1}H_2{}^{2}H$ and $^{13}C^{1}H^{2}H_2$ methyl isotopomers, respectively. Cavanagh et al. [13] provide a comprehensive summary of contemporary multidimensional pulse sequences used to measure ^{2}H, ^{13}C and ^{15}N relaxation rates of proteins in solution, along with citations to original publications.

About 20 years ago, Cole and Torchia [33] reported ^{15}N R_1 values of several types of amino acids in crystalline staphylococcal nuclease, measured using 1D cross polarization MAS (CPMAS) NMR. In 2004, Giraud [34] reported ^{15}N R_1 values at sequentially assigned sites throughout crystalline $^{13}C/^{15}N$ labeled Crh, measured using two-dimensional ^{13}C–^{15}N CPMAS. The number of solid-state measurements of ^{2}H, ^{13}C and ^{15}N relaxation rates at individual sites throughout uniformly labeled proteins has increased rapidly since that time [35]. As in solution, pulse sequences have been developed that measure R_1, $R_{1\rho}$, and the heteronuclear NOE. In solids, internal motions alone determine relaxation rates, which are therefore sensitive to dynamics on a timescale of microseconds to picoseconds. While relaxation measurements in solids sample a far wider range of internal motions than in liquids, large-amplitude slow motions can severely attenuate the efficiency of cross-polarization (CP) transfer, and greatly reduce sensitivity. This problem has been addressed by recording spectra of perdeuterated proteins in which approximately 20% of the labile hydrogen atoms are back-exchanged with protons. The reduction in transverse relaxation rates, resulting from the combination of deuteration, high speed MAS and TROSY selection, enables one to use INEPT-type transfers (as done in solution) to observe signals from spins in regions of proteins undergoing large-amplitude slow dynamics, where experiments based on CP dipolar-transfers fail [36]. Experiments incorporating high speed MAS have also been used to measure deuterium relaxation of ^{2}H labeled methyl groups in proteins, although MAS-driven spin diffusion can complicate data analysis [37].

5. Extracting information about dynamics from relaxation data

In solution, spectral densities are functions of overall (τ_c) and internal (τ_i) correlation times [38–41], where $\tau_i < \tau_c$. So, in contrast with relaxation measurements in solids, relaxation measurements in solution provide typically provide information about internal motions in proteins on a timescale of less than a few nanoseconds, i.e., faster than overall rotational motion.

Early relaxation measurements on peptides and proteins in solution were often analyzed using specific models for molecular reorientation, typically rotational diffusion for overall reorientation and diffusive or jump models for internal motion [4,5,38,39,42]. Although Wittebort and Szabo [40] derived equations for relaxation rates for spins in amino-acid sidechains undergoing complex internal motions, the extensive relaxation data needed to determine the many unknown rates and amplitudes that enter their expression for $J(\omega)$ are typically not available. In the usual case, where data are insufficient to specify a unique model of dynamics, the model-free approach (MFA) [43,44] is widely applied to characterize dynamics in terms of a generalized order parameter, S^2, and overall and effective internal correlation times, τ_c and τ_e, respectively. In the case of the I–S dipolar relaxation between two spin-1/2 nuclei, the MF expression for $J(\omega)$ is

$$J(\omega) = (2/5)[S^2\tau_c/(1+\omega^2\tau_c^2) + (1-S^2)\tau/(1+\omega^2\tau^2)]$$
$$S^2 = \sum_{m=-2}^{2} |\langle C_{2m}(\theta,\phi)\rangle|^2; \quad 1/\tau = 1/\tau_c + 1/\tau_e, \tag{2}$$

where C_{2m} are modified spherical harmonics, (θ, ϕ) are polar angles that define the orientation of the I–S bond relative the molecular frame, and the angular brackets denote an average over orientations on a timescale shorter than approximately τ_c [43]. The MFA expression is exact when overall motion is isotropic, $\tau_e \ll \tau_c$, ω^{-1}, and internal and overall motions are uncoupled. Although the accuracy of the MFA outside these limits has been questioned [45], the current consensus is that the MF expression for $J(\omega)$ remains a good approximation outside its strict range of applicability [46,47].

One circumstance where the MFA is not applicable, because internal and overall motions are coupled, occurs when an internal motion involves a large domain whose movement changes the overall rotational diffusion of a biomolecule [48]. This occurs commonly for RNA molecules, which are often highly flexible, complicating analysis of relaxation data as well as RDC data (see below), and thereby obscuring functional dynamics of RNA. The decoupling of internal and overall motions has been achieved by using the domain-elongation approach in which the labeled RNA of interest is covalently linked to much larger and unlabeled double-helical A-RNA [49,50]. The overall motion of the assembly is typically slower than the internal motion of the labeled RNA and little affected by it. This enables the internal motion of the RNA to be characterized using MFA.

In solids, where overall reorientation is absent, only the second term in Eq. (2) contributes to $J(\omega)$ and the generalized order parameter can be derived from measurement of principal frequencies of averaged anisotropic interactions [51], as discussed below. Once S^2 is known, τ_ε can be obtained from a R_1 measurement, provided motion takes place on a single or narrow range of timescales.

When internal motion takes place on two distinct timescales, the extended MFA can be used to analyze relaxation data [52]. Comparing order parameters and correlation times for the same protein in solution with those in the solid state, opens the way to examine the extent to which the S^2 is reduced by motions on different times scales and to learn about the impact of intermolecular contacts on internal motions of proteins [53].

Spectral densities have been determined directly by measuring relaxation rates over a wide range of magnetic fields using rapid field cycling. Recently this approach has been adapted to study the dynamics of complex biomolecules, which requires recording spectra with high sensitivity and resolution, by a rapid sample shuttling device [54]. With this device, relaxation that occurs at low fields is encoded in magnetization that is established and subsequently detected in the strong homogeneous field of a commercial spectrometer. Redfield and associates have used this approach to measure ^{15}N and ^{31}P relaxation in biomolecules [55–58] at field strengths spanning more than two orders of magnitude, demonstrating the feasibility of wide-range spectral density mapping in solution with high spectral resolution.

Protein spectral density has also been mapped using relaxation measurements made solely at high fields [59,60]. The ease of extracting approximate information about biomolecular dynamics using the MFA has resulted in its widespread use; however, spectral density mapping is an important alternative approach that does not require the approximations of the MFA. It therefore has the potential to provide a more direct means of comparing experimental measurements with predictions of molecular dynamics (MD) simulations.

6. Extracting information about dynamics from residual anisotropic interactions

In a static solid, the resonance frequency depends upon the orientation of an anisotropic tensor interaction (one of those discussed in Section 3) with respect to B_o. As a consequence of this angular dependence, NMR spectra in solids typically display broad powder patterns, like that shown in Fig. 2A for a spin-1/2 nucleus like ^{15}N spin that is dipolar coupled to a single proton. In this case the interaction tensor is axially symmetric with the unique axis along the NH bond, and the orientation dependence of the resonance frequency is given by

$$\omega(\theta_L) = \pm\omega_{DD}P_2(\cos\theta_L) \tag{3}$$

The sign depends upon the spin state of the proton (α or β), and θ_L is the angle made by the NH bond axis and B_o. The dipolar coupling, in Hz, for each value of θ_L is the difference between $\omega(\alpha)$ and $\omega(\beta)$ i.e. equals $-\omega_{DD}P_2(\cos\theta_L)/\pi$. In solution where $\tau_c \ll 1/\omega_{DD}$ the residual dipolar coupling, RDC (in Hz) is given by the ensemble average [61]

$$\mathrm{RDC} = D_m\langle P_2(\cos\theta_L)\rangle \tag{4}$$

where $D_m = -\omega_{DD}/\pi$. Using the addition theorem of spherical harmonics one obtains

$$\mathrm{RDC} = D_m\sum_{m=-2}^{2}\langle C^*_{2m}(\Theta,\Phi)\rangle\langle C_{2m}(\theta,\phi)\rangle \tag{5}$$

where (Θ, Φ), (θ, ϕ) are polar angles that define the orientations of the external field, B_o, and the N–H bond axis in a molecule fixed frame, respectively, and it is assumed that the ensemble averages over (Θ, Φ) and (θ, ϕ) are uncorrelated. The ensemble averages over (Θ, Φ) are related to Saupe order-matrix elements and vanish in the absence of alignment. However this is not the case if an anisotropic medium is used to align a biomolecule with respect to B_o. A RDC is then observed in the solution spectrum, Fig. 3A. Choosing the axes

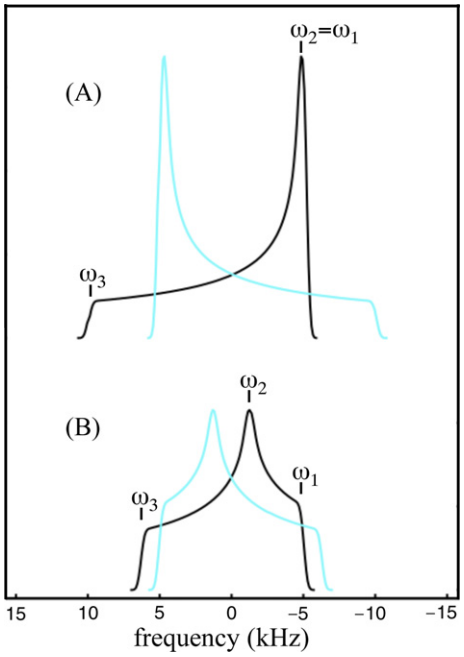

Fig. 2. (A) Solid state NMR spectrum of a spin-1/2 nucleus, e.g. ^{15}N, that has a dipolar interaction with a single ^{1}H spin ($-\omega_{DD}/\pi$ = 20 kHz, chemical shift anisotropy is not considered). Two powder patterns, the "Pake doublet" are seen, corresponding to the two spin-states (α and β) of the proton. The frequency distribution manifest in each pattern results from the angular dependence of the resonance frequency, Eq. (3). The positions of principal frequencies (ω_1, ω_2, ω_3) are indicated by short vertical lines. The maximum frequency, ω_3, corresponds to the NH bond parallel to B_o, while the minimum frequencies $\omega_1 = \omega_2 = -\omega_3/2$ result when the NH bond is perpendicular to B_o. In the absence of motion, the maximum dipolar splitting, $D_m = \omega_3/\pi$, is 20 kHz. (B) Reorientation of the NH bond with $\tau_i < \omega_3$ averages the frequency distribution, resulting in a contraction of the static powder pattern. For example if the N–H bond alternates between two equally populated orientations which differ by 60°, the averaged powder pattern seen at the bottom of the figure is the result. The asymmetric motion lifts the degeneracy in the principal frequencies and yields an axially asymmetric powder pattern. A comparison of principal frequencies in (A) with (B) allows the value of S^2 to be calculated [51]. In similar fashion, S^2 can be derived from dynamically averaged spin-1/2 chemical shift and ^{2}H quadrupolar powder patterns. Contemporary high-resolution solid-state experiments are typically recorded with MAS. Although fast MAS averages each powder line shape to a single line, at the frequency of the isotropic chemical shift, numerous approaches, noted in the text, are available that recover the information contained in the anisotropic line shapes, while retaining the high resolution provided by MAS.

of the molecule-fixed frame to be the principal axes of the alignment tensor, the RDC is given by [61]

$$\mathrm{RDC} = (D_m/2)A_a[3\cos^2\theta - 1 + \eta_a\sin^2\theta\cos 2\phi] \tag{6}$$

where A_a and η_a are the magnitude and asymmetry of the alignment tensor. In studies of biomolecules, anisotropic media that produce very weak alignment, $A_a \sim .001$, are employed in order to record simple spectra from which short-range dipolar couplings can readily be measured [61]. Therefore, as seen by comparing Figs. 2A and 3A, RDCs are typically 1000-fold smaller than dipolar couplings in static solids.

The use of anisotropic media opened the way to measure residual dipolar, CSA and quadrupolar interactions at sites throughout biomolecules in solution. RDCs and RCSAs have provided long range orientational constraints that have greatly increased the power of NMR to solve structures of proteins and nucleic acids, and have also significantly improved the accuracy of such structures [62]. In addition to providing structural information, RDCs have also yielded information about internal dynamics [63,64].

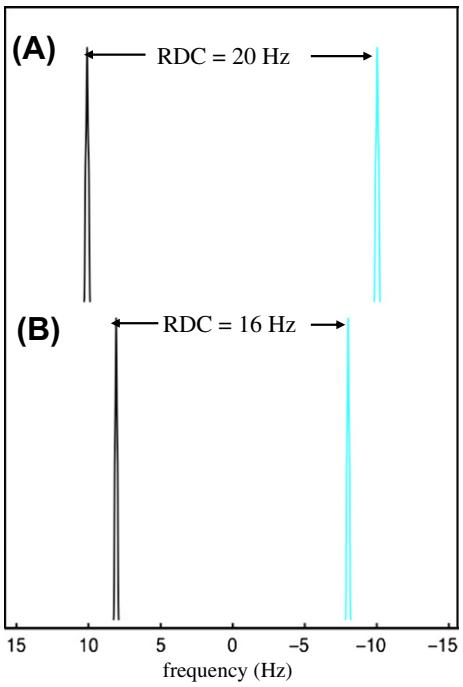

Fig. 3. In solution rapid overall tumbling, $\tau_c < 10^{-6}$ s, causes the right side of Eq. (4) to vanish, eliminating all RDCs. However this is not the case for an aligned sample, because of the non-random distribution of NH bond orientations with respect to B_o, and RDCs are given by Eq. (6). (A) Shows the maximum RDC, 20 Hz, obtained assuming $D_m = 20$ kHz, weak alignment, $A_a = .001$, with $\theta = 0°$. Other NH orientations will exhibit smaller RDCs, whose values also depend upon η_a. (B) Illustrates the reduction in the RDC shown in (A) that results from diffusion ($\tau_i < 10^{-4}$ s) of the NH bond in a cone having semi-angle 30°, for which $S = 0.8$.

Internal motions on the timescale of less than about 10^{-4} s, diminish the ensemble averages of (θ, ϕ) in Eq. (5) and thereby reduce RDCs, as depicted in Fig. 3B. Under certain assumptions, these ensemble averages, which are related to S^2 according to Eq. (2), can be determined when RDCs are measured for many I–S bonds in five independent alignments [63,64]. In this case, analysis of RDCs yields order parameters S and η ($S = \sqrt{S^2}$, where S^2 is the Lipari–Szabo order parameter defined in Eq. (2) and η is the asymmetry parameter) that characterize the amplitude and asymmetry of the motion, respectively, as well as the Euler angles that describe the orientation of the principal axis system of the averaged dipolar tensor, in a model-independent manner. Similar information is obtained from the analysis of averaged anisotropic interactions in solids [51]. If internal motions are approximately axially symmetric, dynamics can be characterized using RDCs measured in three independent alignments [65,66], However, note that when internal motions affect the overall shape and alter the alignment tensor of a biomolecule, it is much more difficult to analyze RDC data, as is the case with relaxation data when internal and overall motions are coupled.

In solution, RDCs are sensitive to much slower internal motions than are spin relaxation rates and several studies have compared order parameters obtained from the two types of measurements in order to extract information about internal motions on the μs-ms timescale. In making such comparisons, the same values of ω_{DD} must be used to analyze both types of experimental data and the S values obtained from RDC data must be normalized [67], because the absolute degree of alignment, A_a in Eq. (6), is unknown. The latter has been done using two distinct approaches [66–68].

One caveat regarding the interpretation of a large order parameter is worth noting. Although it is widely recognized that S^2 is insensitive to a small-amplitude motion, a large-amplitude motion involving a state with a small population also has little impact on the observed order parameter. As an example, if an N–H bond axis jumps between two orientations, which differ by an angle θ_{ab}, with relative populations p_a and p_b, then S^2 is given by [43]

$$S^2 = 1 - 3p_a p_b \sin^2 \theta_{ab} \tag{7}$$

Clearly, S^2 approaches unity for all θ_{ab} when $p_a p_b$ is small. Therefore only a small reduction in S will result from a dynamic process involving a state with a small relative population, making such a transition difficult to detect.

In solids, principal frequencies derived from dynamically averaged powder lineshapes, Fig. 2B, directly yield information about order parameters characterizing motions of internuclear vectors (or more properly, interaction tensor principal axes) that are on timescales of less than about 10^{-4}–10^{-6} s, depending upon the magnitude of the static tensor [51]. CSA tensor principal components have been measured at sites throughout proteins using slow MAS as well as CSA recoupling techniques [69], while dipolar tensor components have been measured using REDOR [70], phase-inverted CP [71] or Lee-Goldburg [72] approaches to recouple dipolar interactions. As noted above, order parameters obtained from averaged interaction tensors in solids can be used in conjunction with relaxation rates to characterize the internal dynamics throughout biomolecules, on timescales ranging from microseconds to picoseconds. For example, the sensitivity of ^{2}H powder lineshapes and ^{13}C relaxation rates to motions on different timescales has been used to reveal dynamics on both μs and ns timescales at functionally important recognition sites in TAR RNA [73].

7. Dynamics on the ms–μs timescale

The sensitivity of NMR lineshapes to motions on the ms–μs timescale provided chemists with one of the first NMR tools to study chemical (conformational) exchange in solution and solid states [74]. The introduction of pulsed NMR, together with CPMG and spin-lock approaches made it possible to measure rates of transverse relaxation in the time domain as a function of the effective radio frequency (RF) field strength; that is, to measure relaxation dispersion (RD) profiles. RD profiles of ^{1}H, ^{13}C and ^{15}N spins in amino acid residues throughout uniformly labeled proteins can be recorded by incorporating either CPMG or spin-lock elements into 2D heteronuclear NMR experiments [75–77]. The relaxation-compensated CPMG approach [78] enables accurate values of the exchange contribution to R_2, R_{ex}, to be measured over a wide range of effective fields, while incorporation of a constant-time relaxation period reduces the time required to measure a RD profile and removes the effect of non-exponential R_2 relaxation on measurement of R_{ex} [79]. In the case of two-site exchange, R_{ex} depends upon the exchange rate, k_{ex}, the site populations, the chemical shift difference between the sites ($\Delta\omega$) and the effective RF field. Measuring R_{ex} as a function of the effective RF field provides RD profiles for spins throughout a protein. By recording data at two (or more) B_o strengths it is often possible to determine all of the chemical exchange parameters. This has been achieved for three-site exchange [76] as well. Amide- and methyl-TROSY approaches [80,81] have been used to record RD profiles and investigate functional conformational exchange of large proteins and supra-molecular complexes, respectively – the latter having molecular weights approaching 1 MDa [82].

The power-handling capacity of NMR probes limits the maximum effective field strengths in CPMG experiments to the range of about 1–4 kHz, depending upon the type of spin, whereas 4- to 5-fold larger fields can be applied in $R_{1\rho}$ measurements. For this reason, fast dynamic processes, particularly those in the fast exchange limit, are

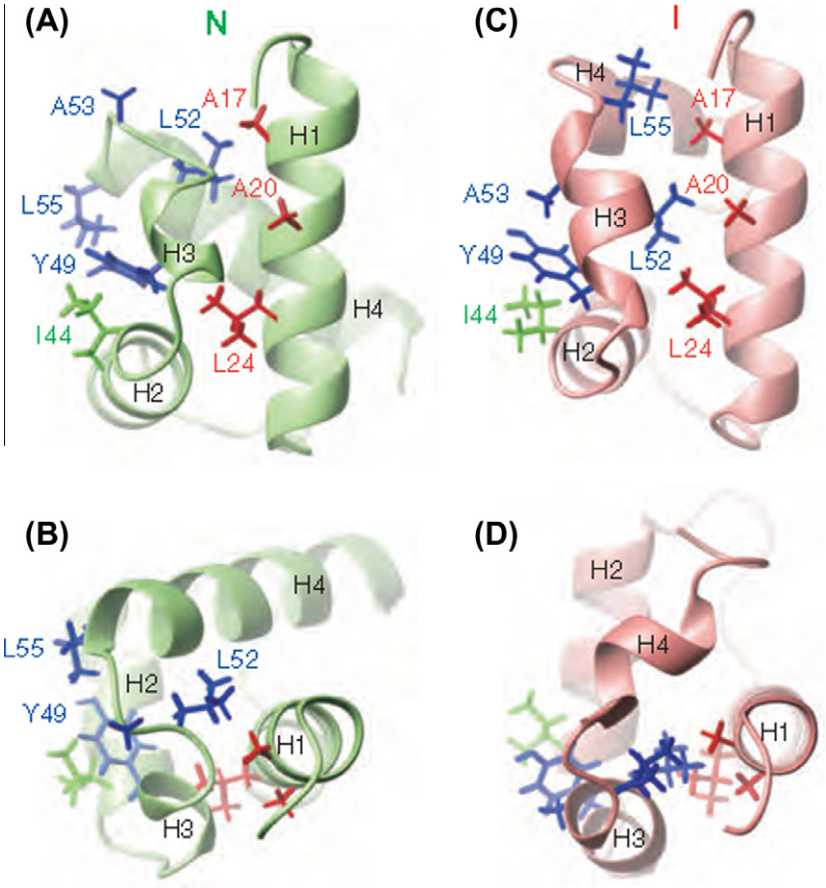

Fig. 4. Non-native interactions in the intermediate state (I) observed [83] on the folding pathway of the FF domain of protein HYPA/FBP11. Structure and packing in the folding intermediate, pink in (C and D), as compared with the native protein (N), light green in (A and B). The skeletal structures of side chains of residues from helices H1 (red), H2 (green) and H3 (blue) that form non-native contacts in the intermediate state are shown. Structures (B and D) are rotated by 90° relative to (A and C), respectively. From, D.M. Korzhnev, T.L. Religa, W. Banachewicz, A.R. Fersht, L.E. Kay, A transient and low-populated protein-folding intermediate at atomic resolution, Science 329 (2010) 1312–1316. Reprinted with permission from AAAS.

typically studied by recording $R_{1\rho}$ RD profiles. Recently, advances in both the theory and measurement of $R_{1\rho}$ outside the fast limit, and using a wide range of spin lock fields, [75] have made it possible to study slow dynamic processes using $R_{1\rho}$ RD.

Although the magnitude of R_{ex} diminishes when exchange involves a highly populated (ground) state and a sparsely populated excited state (or states), the high sensitivity of heteronuclear NMR spectra enables accurate measurement of RD profiles that have small amplitudes. Hence, RD experiments have provided chemical shifts of excited states of biomolecules that have populations as low as 0.5%. Such states are difficult to detect by non-NMR techniques and are typically too weak to observe directly in NMR experiments, hence the name "invisible" states [76]. Recently the high-resolution structure of such a state, a transient protein folding intermediate (population ca. 3%), depicted in Fig. 4, was solved by supplying the chemical shifts of the invisible intermediate to the structure prediction program, CS-Rosetta [83]. RDCs and RCSAs of invisible states have also been measured, and the combination of chemical shift, RDC, and RCSA restraints has been used to solve the structures of invisible states [76].

In the limit of very fast two-site exchange, $k_{ex}^2 \gg \Delta\omega^2$, the maximum value of R_{ex} observed in both CPMG and $R_{1\rho}$ experiments is given by

$$R_{ex}^{\max} = p_a p_b \Delta\omega^2 / k_{ex} \tag{8}$$

According to Eq. (8) the maximum amplitude of CPMG and $R_{1\rho}$ dispersion profiles diminishes as k_{ex} increases, making it difficult to detect rapid exchange processes, particularly those involving states with small populations. Recently it has been shown that measurements of proton paramagnetic relaxation enhancements (PREs) can detect conformational exchange, involving a minor state, which is too fast to detect using CPMG experiments [84]. The PRE is proportional to the inverse sixth power of the proton–electron distance so that the linewidth of the detected signal increases significantly for each site having a proton–electron distance in the minor conformation that is significantly smaller than in the major conformation.

8. Dynamics on the timescale of ms and beyond

The 2D magnetization exchange experiment [85] is well suited to study slow conformational exchange. Exchange rates in the range of about 0.2–50 s^{-1} can be measured, with the lower and upper limits determined by the longitudinal relaxation rate and by peak broadening, respectively. Early applications measured exchange of ^1H magnetization to follow slow conformational exchange of small molecules. Because both ^1H cross relaxation and exchange cause transfer of ^1H z-magnetization in biomolecules, exchange rates of either ^{15}N z-magnetization or of $^1H/^{15}N$ two-spin order are more straightforward to interpret, and are commonly measured when ^{15}N labeled biomolecules are available. These types of experiments have been applied to measurements of slow exchange in increasingly complex systems [86] having molecular weights up to 300 kDa [77].

Measurement of hydrogen–deuterium exchange in solution was among the earliest methods used to demonstrate the dynamic nat-

ure of proteins [87]. Conformational fluctuations involving the breaking of hydrogen bonds within proteins, on the timescale of ms to hours, have been monitored using a variety of NMR experiments that measure the rate of exchange of amide protons with water protons or deuterons [88]. A novel ultra-fast method for acquiring 2D spectra has been used to directly record hydrogen–deuterium exchange rates of the order of a few seconds [89]. Minutely populated states along the protein-folding pathway have been observed using hydrogen–deuterium exchange experiments carried out under native-state conditions [90]. Quantitative measurements of H–D exchange rates in proteins, under equilibrium conditions, have recently been extended to solids [91].

9. Relating biomolecular dynamics to function

Numerous NMR studies have convincingly shown that biomolecules exhibit conformational fluctuations spanning a wide range of timescales. These motions include ubiquitous small amplitude movements, larger amplitude motions of chain segments and of sidechains, and conformational changes encompassing structural domains or entire molecules. In the event that the function of a biomolecule is known, the dynamics information provided by NMR often provides insights about the mechanistic basis for function, as a few examples discussed below illustrate.

The crystal structure of calmodulin revealed two globular domains connected by a highly ordered helix. In spite of its high quality, the structure did not indicate how calmodulin could bind to numerous different target molecules. ^{15}N spin relaxation measurements revealed that the middle of the helix was flexible [92], suggesting that a flexible hinge in the helix played an important role in binding targets. This was confirmed by subsequent NMR and crystal structures that revealed a sharp bend in the helix of calmodulin bound to various targets. Crystal structures of HIV protease showed that a pair of β-sheets, called the flaps, block access of natural substrates to the active site. Both ^{15}N spin relaxation and CPMG measurements revealed that the tips of flaps are flexible gates that permit access to the catalytic site [93,94].

NMR studies have identified dynamics that reveal mechanisms underlying biomolecular recognition. An analysis of ubiquitin RDCs measured in multiple alignments reveals a dynamic ensemble of protein conformations that span the range of structures of ubiquitin bound to various protein targets [95], suggesting that recognition of ubiquitin involves selection from the apo-state ensemble, rather than by induced fit. In contrast, chemical shift and CPMG-RD data showed that a helix in the pKID domain folds fully only when binding to the KIX domain is complete, an example of the induced fit binding mechanism [96]. PRE measurements have shown that the HoxD9 homodomain efficiently recognizes its specific DNA binding site by diffusing along the DNA double helix [97].

The dynamics and pathways of protein and RNA folding have been intensively investigated in the past decade. Although protein folding is often described as a two-state process involving an unfolded and a fully-folded molecule, NMR CPMG-RD and H-exchange studies in solution have identified intermediate states, sparsely populated at thermal equilibrium, along the folding pathway, some stabilized by native and others by non-native interactions [76]. A solid-state NMR freeze-quench experiment [98] has shown that the rapid folding of the villin headpiece involves an intermediate state having secondary structure of the folded state, but incomplete tertiary structure, as illustrated in Fig. 5. Detailed analyses of extensive sets of NMR data, particularly RDCs and PREs, show that the dynamic ensemble of conformations that comprise the unfolded "state" of a protein often deviates significantly from that of a random coil [99]. The observation of structural preferences in the unfolded state helps explain the rapidity with which proteins fold and the activity of natively unfolded proteins. Methyl-TROSY has been used to elucidate the role played by dynamics of methyl-containing amino acids in the function of the 20S proteasome, a 670 kD supramolecular protein assembly. A variety of ^{1}H and ^{13}C spin relaxation measurements, including PREs, together with strategically placed mutations indicate that control of proteolysis is achieved by a dynamic gate at the N-termini of the proteosome α-subunits [82].

10. Exploiting multiple biophysical approaches to characterize dynamics

While this article has focused on the various NMR methodologies that are available to study the dynamics of proteins and nucleic acids, biomolecular dynamics is clearly very complex, and a complete description of dynamics requires the specification of positions of thousands of atoms as a function of time. NMR provides information about aspects of this complex process that complements information obtained using other biophysical techniques. Indeed, the synergistic relationship of NMR spectroscopy with other biophysical approaches is widely recognized and increasingly exploited to study biomolecular structure and dynamics. The Biological Magnetic Resonance Bank (BMRB) [100] provides convenient access to a large database of experimental NMR parameters and restraints that have been collected for thousands of proteins and nucleic acids. Protein relaxation data were first used to test dynamics simulations nearly 30 years ago [101], and the BMRB provides the opportunity for comprehensive testing of the force fields used to calculate configurational energies and MD trajectories of biomolecules [102,103]. From the reverse perspective, im-

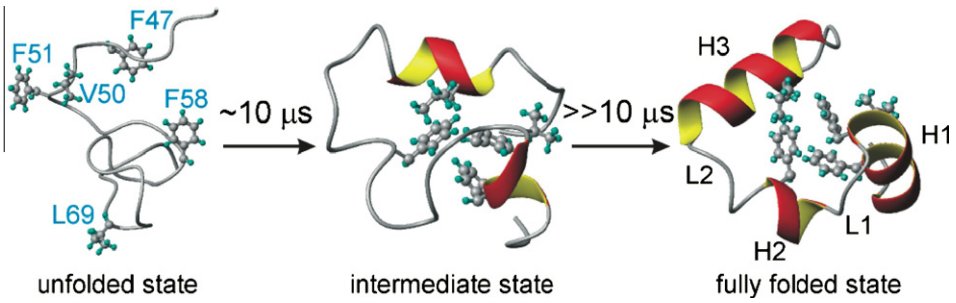

Fig. 5. Schematic illustration of the villin headpiece, HP35, folding process. Starting with a thermally unfolded ensemble that lacks helical secondary structure, a rapid temperature drop causes rapid conversion to an intermediate ensemble with nearly native secondary structure but disordered tertiary structure. The fully folded state, with helical segments joined by ordered loops and with an ordered hydrophobic core, forms on a longer timescale. Reprinted with permission from, K.N. Hu, W.M. Yau, R. Tycko, Detection of a transient intermediate in a rapid protein folding process by solid-state nuclear magnetic resonance, J. Am. Chem. Soc. 132 (2010) 24–25. Copyright, 2010, American Chemical Society.

proved computational approaches have enabled accurate prediction of protein structures with limited amounts of readily acquired NMR data [104–106].

A few recent examples will serve to illustrate how combining NMR with other biophysical approaches has been used to relate dynamics with function: RD measurements together with MD simulations reveal that a small population of Hoogsteen base pairs is in dynamic equilibrium with Watson–Crick base pairs in free double-stranded DNA [107]. This observation indicates that considerable structural diversity, well beyond the Watson–Crick double helix, underlies DNA function. MD calculations, X-ray, FRET, and CPMG NMR all provided crucial information that culminated in a model for the dynamics trajectory that connects the open and (catalytically competent) closed states of adenylate kinase [108]. As noted earlier, CPMG-RD NMR is a powerful means of identifying protein folding intermediates; nonetheless, full characterization of such states benefits from inclusion of chemical shift–directed structure prediction, mutational analysis, and optical measurements of folding kinetics [83]. Numerous biophysical approaches, including prominent contributions made by solution- [109] and solid-state [110,111] NMR, have contributed to our emerging understanding of the intricate proton transport mechanism of the influenza virus M2 channel [112]. Fuller insight into this mechanism will come from further biophysical studies of the dynamics of functional sidechains and water molecules within the M2 channel [112], an enterprise in which NMR is well-suited to play a major role.

11. Future prospects for NMR studies of biomolecular dynamics

Advances in segmental and tailored labeling that simplify spectra of biomolecules promise to enable spectral assignment and dynamics studies of increasingly complex biomolecules, both in solution and in the solid state. Many new reagents have been introduced that allow for site-specific attachment of paramagnetic metal ions to diamagnetic proteins and nucleic acids. These developments open possibilities for acquiring of RDC, PRE and pseudo contact shift data that would complement data acquired for the diamagnetic biomolecule. In solids, paramagnetic enhanced ^{1}H relaxation combined with fast MAS holds promise for the increasing sensitivity of relaxation measurements by reducing the acquisition recycle delay.

Solution and solid-state measurements of interaction tensor components will continue to improve knowledge of how these fundamental NMR parameters depend upon residue-type and the local chemical and structural environment. The novel solid-state NMR methods for studying biomolecular dynamics that have been developed on small microcrystalline proteins should soon find exciting applications in studies of the functional dynamics of membrane proteins and fibrous proteins implicated in various neurological diseases. It also seems likely that the methodology used to obtain sequential assignments of uniformly labeled proteins in the solid-state will be extended to assign labeled RNAs, making them amenable to dynamics characterization. The inclusion of chemical shifts in structure prediction schemes will likely be increasingly exploited to uncover on- and off-pathway states involved in protein folding, while improved computational procedures, when applied to analyze all types of NMR data that are sensitive to conformational averaging, will better characterize the complex ensembles of states that comprise intrinsically unfolded, but functional, proteins.

As is well appreciated, identifying the role of structural dynamics in a complex biological mechanism is a formidable undertaking that requires combined application of numerous approaches. NMR has played prominent role in this enterprise and, given the developments that appear on the horizon, will likely continue to play an increasingly important one.

Acknowledgment

I thank Ad Bax, Nicolas Fawzi and Attila Szabo for numerous helpful suggestions. This article is dedicated to Lewis Kay on the occasion of his fiftieth birthday.

References

[1] A. Abragam, The Principles of Nuclear Magnetism, Oxford University Press, Oxford, UK, 1961.
[2] A. Allerhand, D. Doddrell, U. Glushko, D.W. Cochran, E. Wenkert, P.J. Lawson, F.R.N. Gurd, Carbon-13 Fourier transform nuclear magnetic resonance. 3. Conformation and segmental motion of native and denatured ribonuclease-A in solution – application of natural-abundance carbon-13 partially relaxed Fourier transform nuclear magnetic resonance, J. Am. Chem. Soc. 93 (1971) 544–546.
[3] E. Oldfield, R.S. Norton, A. Allerhand, Studies of individual carbon sites of proteins in solution by natural abundance carbon 13 nuclear magnetic-resonance spectroscopy – relaxation behavior, J. Biol. Chem. 250 (1975) 6368–6380.
[4] R. Richarz, K. Nagayama, K. Wuthrich, C-13 nuclear magnetic-resonance relaxation studies of internal mobility of the polypeptide-chain in basic pancreatic trypsin-inhibitor and a selectively reduced analog, Biochemistry 19 (1980) 5189–5196.
[5] R.J. Wittebort, T.M. Rothgeb, A. Szabo, F.R.N. Gurd, Aliphatic groups of sperm whale myoglobin – C-13NMR-study, Proc. Natl. Acad. Sci. USA 76 (1979) 1059–1063.
[6] G. Wagner, A. Demarco, K. Wuthrich, Dynamics of aromatic amino-acid residues in globular conformation of basic pancreatic trypsin-inhibitor (BPTI). 1. H-1 NMR-studies, Biophys. Struct. Mech. 2 (1976) 139–158.
[7] G. Wagner, A topical issue: production and labeling of biological macromolecules for NMR investigations, J. Biomol. NMR 46 (2010) 1–2.
[8] R.T. Batey, J.L. Battiste, J.R. Williamson, Preparation of isotopically enriched RNAs for heteronuclear NMR, Methods Enzymol. 261 (1995) 300–322.
[9] K. Lu, Y. Miyazaki, M.F. Summers, Isotope labeling strategies for NMR studies of RNA, J. Biomol. NMR 46 (2010) 113–125.
[10] X.C. Su, G. Otting, Paramagnetic labelling of proteins and oligonucleotides for NMR, J. Biomol. NMR 46 (2010) 101–112.
[11] L.G. Werbelow, D.M. Grant, Intramolecular dipolar relaxation in multispin systems, in: J.A. Waugh (Ed.), Advances in Magnetic Resonance, Academic Press, Inc., New York, 1977, pp. 190–299.
[12] M. Goldman, Interference effects in the relaxation of a pair of unlike spin-1/2 nuclei, J. Magn. Reson. 60 (1984) 437–452.
[13] J. Cavanagh, W.J. Fairbrother, A.G. Palmer, M. Rance, N.J. Skelton, Protein NMR Spectroscopy: Principles and Practice, second ed., Academic Press, San Diego, 2006.
[14] K.W. Waddell, E.Y. Chekmenev, R.J. Wittebort, Single-crystal studies of peptide prolyl and glycyl N-15 shielding tensors, J. Am. Chem. Soc. 127 (2005) 9030–9035.
[15] H. Saito, I. Ando, A. Ramamoorthy, Chemical shift tensor – the heart of NMR: insights into biological aspects of proteins, Prog. Nucl. Magn. Reson. Spectrosc. 57 (2010) 181–228.
[16] B.J. Wylie, L.J. Sperling, H.L. Frericks, G.J. Shah, W.T. Franks, C.M. Rienstra, Chemical-shift anisotropy measurements of amide and carbonyl resonances in a microcrystalline protein with slow magic-angle spinning NMR spectroscopy, J. Am. Chem. Soc. 129 (2007) 5318–5319.
[17] G. Cornilescu, A. Bax, Measurement of proton, nitrogen, and carbonyl chemical shielding anisotropies in a protein dissolved in a dilute liquid crystalline phase, J. Am. Chem. Soc. 122 (2000) 10143–10154.
[18] L.S. Yao, A. Grishaev, G. Cornilescu, A. Bax, Site-specific backbone amide N-15 chemical shift anisotropy tensors in a small protein from liquid crystal and cross-correlated relaxation measurements, J. Am. Chem. Soc. 132 (2010) 4295–4309.
[19] B.J. Wylie, C.D. Schwieters, E. Oldfield, C.M. Rienstra, Protein structure refinement using C-13-alpha chemical shift tensors, J. Am. Chem. Soc. 131 (2009) 985–992.
[20] L.S. Yao, B. Vogeli, J.F. Ying, A. Bax, NMR determination of amide N–H equilibrium bond length from concerted dipolar coupling measurements, J. Am. Chem. Soc. 130 (2008) 16518–16520.
[21] M. Ottiger, A. Bax, Determination of relative N–H–N N–C′, C-alpha-C′, and C(alpha)–H-alpha effective bond lengths in a protein by NMR in a dilute liquid crystalline phase, J. Am. Chem. Soc. 120 (1998) 12334–12341.
[22] M. Ottiger, A. Bax, How tetrahedral are methyl groups in proteins? A liquid crystal NMR study, J. Am. Chem. Soc. 121 (1999) 4690–4695.
[23] A. Mittermaier, L.E. Kay, Measurement of methyl – H-2 quadrupolar couplings in oriented proteins. How uniform is the quadrupolar coupling constant?, J Am. Chem. Soc. 121 (1999) 10608–10613.
[24] A. Grishaev, L.S. Yao, J.F. Ying, A. Pardi, A. Bax, Chemical shift anisotropy of imino N-15 nuclei in Watson–Crick base pairs from magic angle spinning

liquid crystal NMR and nuclear spin relaxation, J. Am. Chem. Soc. 131 (2009) 9490–9491.
[25] D.L. Bryce, A. Grishaev, A. Bax, Measurement of ribose carbon chemical shift tensors for A-form RNA by liquid crystal NMR spectroscopy, J. Am. Chem. Soc. 127 (2005) 7387–7396.
[26] J.F. Ying, A. Grishaev, D.L. Bryce, A. Bax, Chemical shift tensors of protonated base carbons in helical RNA and DNA from NMR relaxation and liquid crystal measurements, J. Am. Chem. Soc. 128 (2006) 11443–11454.
[27] J.F. Ying, A.E. Grishaev, A. Bax, Carbon-13 chemical shift anisotropy in DNA bases from field dependence of solution NMR relaxation rates, Magn. Reson. Chem. 44 (2006) 302–310.
[28] N.R. Nirmala, G. Wagner, Measurement of C-13 relaxation-times in proteins by two-dimensional heteronuclear H-1–C-13 correlation spectroscopy, J. Am. Chem. Soc. 110 (1988) 7557–7558.
[29] L.E. Kay, D.A. Torchia, A. Bax, Backbone dynamics of proteins as studied by N-15 inverse detected heteronuclear NMR spectroscopy: application to staphylococcal nuclease, Biochemistry 28 (1989) 8972–8979.
[30] D.R. Muhandiram, T. Yamazaki, B.D. Sykes, L.E. Kay, Measurement of H-2 T-1 and T-1rho relaxation-times in uniformly C-13 labeled and fractionally H-2-labeled proteins in solution, J. Am. Chem. Soc. 117 (1995) 11536–11544.
[31] O. Millet, D.R. Muhandiram, N.R. Skrynnikov, L.E. Kay, Deuterium spin probes of side-chain dynamics in proteins. 1. Measurement of five relaxation rates per deuteron in C-13-labeled and fractionally H-2-enriched proteins in solution, J. Am. Chem. Soc. 124 (2002) 6439–6448.
[32] R. Ishima, A.P. Petkova, J.M. Louis, D.A. Torchia, Comparison of methyl rotation axis order parameters derived from model-free analyses of H-2 and C-13 longitudinal and transverse relaxation rates measured in the same protein sample, J. Am. Chem. Soc. 123 (2001) 6164–6171.
[33] H.B.R. Cole, D.A. Torchia, An NMR-study of the backbone dynamics of staphylococcal nuclease in the crystalline state, Chem. Phys. 158 (1991) 271–281.
[34] N. Giraud, A. Bockmann, A. Lesage, F. Penin, M. Blackledge, L. Emsley, Site-specific backbone dynamics from a crystalline protein by solid-state NMR spectroscopy, J. Am. Chem. Soc. 126 (2004) 11422–11423.
[35] J.R. Lewandowski, L. Emsley, Relaxation studies of solid biopolymers, in: R.K. Harris, R. Wasylishen (Eds.), Encyclopedia of Magnetic Resonance, John Wiley & Sons, Ltd., Chichester, 2009.
[36] R. Linser, U. Fink, B. Reif, Assignment of dynamic regions in biological solids enabled by spin-state selective NMR experiments, J. Am. Chem. Soc. 132 (2010) 8891–8893.
[37] V. Agarwal, A. Diehl, N. Skrynnikov, B. Reif, High resolution H-1 detected H-1, C-13 correlation spectra in MAS solid-state NMR using deuterated proteins with selective H-1, H-2 isotopic labeling of methyl groups, J. Am. Chem. Soc. 128 (2006) 12620–12621.
[38] D.E. Woessner, Nuclear spin relaxation in ellipsoids undergoing rotational brownian motion, J. Chem. Phys. 37 (1962) 647–654.
[39] D.E. Woessner, B.S. Snowden, G.H. Meyer, Nuclear spin–lattice relaxation in axially symmetric ellipsoids with internal motion, J. Chem. Phys. 50 (1969) 719–721.
[40] R.J. Wittebort, A. Szabo, Theory of NMR relaxation in macromolecules – restricted diffusion and jump models for multiple internal rotations in amino-acid side-chains, J. Chem. Phys. 69 (1978) 1722–1736.
[41] G. Lipari, A. Szabo, Nuclear magnetic-resonance relaxation in nucleic-acid fragments – models for internal motion, Biochemistry 20 (1981) 6250–6256.
[42] R.E. London, Interpretation of C-13 spin-lattice relaxation resulting from ring puckering in proline, J. Am. Chem. Soc. 100 (1978) 2678–2685.
[43] G. Lipari, A. Szabo, Model-free approach to the interpretation of nuclear magnetic resonance relaxation in macromolecules. 1. Theory and range of validity, J. Am. Chem. Soc. 104 (1982) 4546–4559.
[44] G. Lipari, A. Szabo, Model-free approach to the interpretation of nuclear magnetic resonance relaxation in macromolecules. 2. Analysis of experimental results, J. Am. Chem. Soc. 104 (1982) 4559–4570.
[45] E. Meirovitch, Y.E. Shapiro, A. Polimeno, J.H. Freed, Structural dynamics of bio-macromolecules by NMR: the slowly relaxing local structure approach, Prog. Nucl. Magn. Reson. Spectrosc. 56 (2010) 360–405.
[46] K.K. Frederick, K.A. Sharp, N. Warischalk, A.J. Wand, Re-evaluation of the model-free analysis of fast internal motion in proteins using NMR relaxation, J. Phys. Chem. B 112 (2008) 12095–12103.
[47] B. Halle, The physical basis of model-free analysis of NMR relaxation data from proteins and complex fluids, J. Chem. Phys. 131 (2009) 224507–224528.
[48] V. Wong, D.A. Case, A. Szabo, Influence of the coupling of interdomain and overall motions on NMR relaxation, Proc. Natl. Acad. Sci. USA 106 (2009) 11016–11021.
[49] Q. Zhang, X.Y. Sun, E.D. Watt, H.M. Al-Hashimi, Resolving the motional modes that code for RNA adaptation, Science 311 (2006) 653–656.
[50] Q. Zhang, H.M. Al-Hashimi, Domain-elongation NMR spectroscopy yields new insights into RNA dynamics and adaptive recognition, RNA-A Publ. RNA Soc. 15 (2009) 1941–1948.
[51] D.A. Torchia, A. Szabo, The information content of powder lineshapes in the fast motion limit, J. Magn. Reson. 64 (1985) 135–141.
[52] G.M. Clore, A. Szabo, A. Bax, L.E. Kay, P.C. Driscoll, A. Gronenborn, Deviation from the simple two-parameter model-free approach to the interpretation of nitrogen-15 nuclear magnetic relaxation of proteins, J. Am. Chem. Soc. 112 (1990) 4989–4991.
[53] V. Agarwal, Y. Xue, B. Reif, N.R. Skrynnikov, Protein side-chain dynamics as observed by solution- and solid-state NMR spectroscopy: a similarity revealed, J. Am. Chem. Soc. 130 (2008) 16611–16621.
[54] A.G. Redfield, Shuttling device for high-resolution measurements of relaxation and related phenomena in solution at low field, using a shared commercial 500 MHz NMR instrument, Magn. Reson. Chem. 41 (2003) 753–768.
[55] M.F. Roberts, Q.Z. Cui, C.J. Turner, D.A. Case, A.G. Redfield, High-resolution field-cycling NMR studies of a DNA octamer as a probe of phosphodiester dynamics and comparison with computer simulation, Biochemistry 43 (2004) 3637–3650.
[56] M.F. Roberts, A.G. Redfield, High-resolution P-31 field cycling NMR as a probe of phospholipid dynamics, J. Am. Chem. Soc. 126 (2004) 13765–13777.
[57] J.B. Klauda, M.F. Roberts, A.G. Redfield, B.R. Brooks, R.W. Pastor, Rotation of lipids in membranes: Molecular dynamics simulation, P-31 spin-lattice relaxation, and rigid-body dynamics, Biophys. J. 94 (2008) 3074–3083.
[58] M.W. Clarkson, M. Lei, E.Z. Eisenmesser, W. Labeikovsky, A. Redfield, D. Kern, Mesodynamics in the SARS nucleocapsid measured by NMR field cycling, J. Biomol. NMR 45 (2009) 217–225.
[59] N.A. Farrow, O.W. Zhang, A. Szabo, D.A. Torchia, L.E. Kay, Spectral density-function mapping using N-15 relaxation data exclusively, J. Biomol. NMR 6 (1995) 153–162.
[60] N.R. Skrynnikov, O. Millet, L.E. Kay, Deuterium spin probes of side-chain dynamics in proteins. 2. Spectral density mapping and identification of nanosecond time-scale side-chain motions, J. Am. Chem. Soc. 124 (2002) 6449–6460.
[61] A. Bax, G. Kontaxis, N. Tjandra, Dipolar couplings in macromolecular structure determination, Methods Enzymol. 339 (2001) 127–174.
[62] A. Bax, A. Grishaev, Weak alignment NMR: a hawk-eyed view of biomolecular structure, Curr. Opin. Struct. Biol. 15 (2005) 563–570.
[63] J.R. Tolman, A novel approach to the retrieval of structural and dynamic information from residual dipolar couplings using several oriented media in biomolecular NMR spectroscopy, J. Am. Chem. Soc. 124 (2002) 12020–12030.
[64] W. Peti, J. Meiler, R. Bruschweiler, C. Griesinger, Model-free analysis of protein backbone motion from residual dipolar couplings, J. Am. Chem. Soc. 124 (2002) 5822–5833.
[65] K. Ruan, K.B. Briggman, J.R. Tolman, De novo determination of internuclear vector orientations from residual dipolar couplings measured in three independent alignment media, J. Biomol. NMR 41 (2008) 61–76.
[66] L. Yao, B. Vogeli, D.A. Torchia, A. Bax, Simultaneous NMR study of protein structure and dynamics using conservative mutagenesis, J. Phys. Chem. B 112 (2008) 6045–6056.
[67] J.R. Tolman, Protein dynamics from disorder, Nature 459 (2009) 1063–1064.
[68] L. Salmon, G. Bouvignies, P. Markwick, N. Lakomek, S. Showalter, D.W. Li, K. Walter, C. Griesinger, R. Bruschweiler, M. Blackledge, Protein conformational flexibility from structure-free analysis of NMR dipolar couplings: quantitative and absolute determination of backbone motion in ubiquitin, Angew. Chem. 48 (2009) 4154–4157.
[69] B.J. Wylie, C.M. Rienstra, Multidimensional solid state NMR of anisotropic interactions in peptides and proteins, J. Chem. Phys. 128 (2008) 052207–052222.
[70] P. Schanda, B.H. Meier, M. Ernst, Quantitative analysis of protein backbone dynamics in microcrystalline ubiquitin by solid-state NMR spectroscopy, J. Am. Chem. Soc. 132 (2010) 15957–15967.
[71] V. Chevelkov, U. Fink, B. Reif, Accurate determination of order parameters from H-1, N-15 dipolar couplings in MAS solid-state NMR experiments, J. Am. Chem. Soc. 131 (2009) 14018–14022.
[72] J. Lorieau, A.E. McDermott, Order parameters based on (CH)–C-13–H-1, (CH2)-C-13–H-1 and (CH3)-C–13-H-1 heteronuclear dipolar powder patterns: a comparison of MAS-based solid-state NMR sequences, Magn. Reson. Chem. 44 (2006) 334–347.
[73] G.L. Olsen, D.C. Echodu, Z. Shajani, M.F. Bardaro, G. Varani, G.P. Drobny, Solid-state deuterium NMR studies reveal mus-ns motions in the HIV-1 transactivation response RNA recognition site, J. Am. Chem. Soc. 130 (2008) 2896–2897.
[74] H.S. Gutowsky, The coupling of chemical and nuclear magnetic phenomena, in: R.K. Harris, R. Wasylishen (Eds.), Encyclopedia of Magnetic Resonance, John Wiley & Sons, Ltd., Chichester, 2009.
[75] A.G. Palmer, F. Massi, Characterization of the dynamics of biomacromolecules using rotating-frame spin relaxation NMR spectroscopy, Chem. Rev. 106 (2006) 1700–1719.
[76] A.J. Baldwin, L.E. Kay, NMR spectroscopy brings invisible protein states into focus, Nat. Chem. Biol. 5 (2009) 808–814.
[77] A.K. Mittermaier, L.E. Kay, Observing biological dynamics at atomic resolution using NMR, Trends Biochem. Sci. 34 (2009) 601–611.
[78] J.P. Loria, M. Rance, A.G. Palmer, A relaxation-compensated Carr–Purcell–Meiboom–Gill sequence for characterizing chemical exchange by NMR spectroscopy, J. Am. Chem. Soc. 121 (1999) 2331–2332.
[79] F.A.A. Mulder, N.R. Skrynnikov, B. Hon, F.W. Dahlquist, L.E. Kay, Measurement of slow (micros-ms) time scale dynamics in protein side chains by N-15 relaxation dispersion NMR spectroscopy: application to Asn and Gln residues in a cavity mutant of T4 lysozyme, J. Am. Chem. Soc. 123 (2001) 967–975.
[80] A.G. Palmer, M.J. Grey, C.Y. Wang, Solution NMR spin relaxation methods for characterizing chemical exchange in high-molecular-weight systems, Methods Enzymol. 394 (2005) 430–465.
[81] D.M. Korzhnev, K. Kloiber, V. Kanelis, V. Tugarinov, L.E. Kay, Probing slow dynamics in high molecular weight proteins by methyl-TROSY NMR spectroscopy: application to a 723-residue enzyme, J. Am. Chem. Soc. 126 (2004) 3964–3973.

[82] T.L. Religa, R. Sprangers, L.E. Kay, Dynamic regulation of archaeal proteasome gate opening as studied by TROSY NMR, Science 328 (2010) 98–102.
[83] D.M. Korzhnev, T.L. Religa, W. Banachewicz, A.R. Fersht, L.E. Kay, A transient and low-populated protein-folding intermediate at atomic resolution, Science 329 (2010) 1312–1316.
[84] C. Tang, C.D. Schwieters, G.M. Clore, Open-to-closed transition in apo maltose-binding protein observed by paramagnetic NMR, Nature 449 (2007) 1078–1082.
[85] J. Jeener, B.H. Meier, P. Bachmann, R.R. Ernst, Investigation of exchange processes by 2-dimensional NMR-spectroscopy, J. Chem. Phys. 71 (1979) 4546–4553.
[86] D. Sahu, G.M. Clore, J. Iwahara, TROSY-based z-exchange spectroscopy: application to the determination of the activation energy for intermolecular protein translocation between specific sites on different DNA molecules, J. Am. Chem. Soc. 129 (2007) 13232–13237.
[87] A. Hvidt, S.O. Nielsen, Hydrogen exchange in proteins, Adv. Protein Chem. 21 (1966) 287–386.
[88] V. Chevelkov, Y. Xue, D.K. Rao, J.D. Forman-Kay, N.R. Skrynnikov, N-15(H/D)-SOLEXSY experiment for accurate measurement of amide solvent exchange rates: application to denatured DRKN SH3, J. Biomol. NMR 46 (2010) 227–244.
[89] M. Gal, P. Schanda, B. Brutscher, L. Frydman, Ultrasofast HMQC NMR and the repetitive acquisition of 2D protein spectra at Hz rates, J. Am. Chem. Soc. 129 (2007) 1372–1377.
[90] H. Maity, M. Maity, M.M.G. Krishna, L. Mayne, S.W. Englander, Protein folding: the stepwise assembly of foldon units, Proc. Natl. Acad. Sci. USA 102 (2005) 4741–4746.
[91] J.M. Lopez del Amo, U. Fink, B. Reif, Quantification of protein backbone hydrogen–deuterium exchange rates by solid state NMR spectroscopy, J. Biomol. NMR 48 (2010) 203–212.
[92] G. Barbato, M. Ikura, L.E. Kay, R. Pastor, A. Bax, Backbone dynamics of calmodulin studied by N-15 relaxation using inverse detected two-dimensional NMR spectroscopy: the central helix is flexible, Biochemistry 31 (1992) 5269–5278.
[93] R. Ishima, D.I. Freedberg, Y.-X. Wang, J.M. Louis, D.A. Torchia, Flap opening and dimer-interface flexibility in the free and inhibitor bound HIV protease and their implications for function, Structure 7 (1999) 1047–1055.
[94] D.I. Freedberg, R. Ishima, J. Jacob, Y.X. Wang, I. Kustanovich, J.M. Louis, D.A. Torchia, Rapid structural fluctuations of the free HIV protease flaps in solution: relationship to crystal structures and comparison with predictions of dynamics calculations, Protein Sci. 11 (2002) 221–232.
[95] O.F. Lange, N.A. Lakomek, C. Fares, G.F. Schroder, K.F.A. Walter, S. Becker, J. Meiler, H. Grubmuller, C. Griesinger, B.L. De Groot, Recognition dynamics up to microseconds revealed from an RDC-derived ubiquitin ensemble in solution, Science 320 (2008) 1471–1475.
[96] K. Sugase, H.J. Dyson, P.E. Wright, Mechanism of coupled folding and binding of an intrinsically disordered protein, Nature 447 (2007) 1021–1025.
[97] G.M. Clore, J. Iwahara, Theory, practice, and applications of paramagnetic relaxation enhancement for the characterization of transient low-population states of biological macromolecules and their complexes, Chem. Rev. 109 (2009) 4108–4139.
[98] K.N. Hu, W.M. Yau, R. Tycko, Detection of a transient intermediate in a rapid protein folding process by solid-state nuclear magnetic resonance, J. Am. Chem. Soc. 132 (2010) 24–25.
[99] S. Meier, M. Blackledge, S. Grzesiek, Conformational distributions of unfolded polypeptides from novel NMR techniques, J. Chem. Phys. 128 (2008) 052204–052217.
[100] J.L. Markley, E.L. Ulrich, H.M. Berman, K. Henrick, H. Nakamura, H. Akutsu, Biomagresbank (BMRB) as a partner in the worldwide protein data bank (wwPDB): new policies affecting biomolecular NMR depositions, J. Biomol. NMR 40 (2008) 153–155.
[101] G. Lipari, A. Szabo, R.M. Levy, Protein dynamics and NMR relaxation – comparison of simulations with experiment, Nature 300 (1982) 197–198.
[102] D.W. Li, R. Bruschweiler, Certification of molecular dynamics trajectories with NMR chemical shifts, J. Phys. Chem. Lett. 1 (2010) 246–248.
[103] D.W. Li, R. Bruschweiler, NMR-based protein potentials, Angew. Chem. 49 (2010) 6778–6780.
[104] A. Cavalli, X. Salvatella, C.M. Dobson, M. Vendruscolo, Protein structure determination from NMR chemical shifts, Proc. Natl. Acad. Sci. USA 104 (2007) 9615–9620.
[105] Y. Shen, O. Lange, F. Delaglio, P. Rossi, J.M. Aramini, G.H. Liu, A. Eletsky, Y.B. Wu, K.K. Singarapu, A. Lemak, A. Ignatchenko, C.H. Arrowsmith, T. Szyperski, G.T. Montelione, D. Baker, A. Bax, Consistent blind protein structure generation from NMR chemical shift data, Proc. Natl. Acad. Sci. USA 105 (2008) 4685–4690.
[106] S. Raman, O.F. Lange, P. Rossi, M. Tyka, X. Wang, J. Aramini, G.H. Liu, T.A. Ramelot, A. Eletsky, T. Szyperski, M.A. Kennedy, J. Prestegard, G.T. Montelione, D. Baker, NMR structure determination for larger proteins using backbone-only data, Science 327 (2010) 1014–1018.
[107] E.N. Nikolova, E. Kim, A.A. Wise, P.J. O'Brien, I. Andricioaei, H.M. Al-Hashimi, Transient Hoogsteen base pairs in canonical duplex DNA, Nature 470 (2011) 498–502.
[108] K.A. Henzler-Wildman, V. Thai, M. Lei, M. Ott, M. Wolf-Watz, T. Fenn, E. Pozharski, M.A. Wilson, G.A. Petsko, M. Karplus, C.G. Hubner, D. Kern, Intrinsic motions along an enzymatic reaction trajectory, Nature 450 (2007) 838–844.
[109] J.R. Schnell, J.J. Chou, Structure and mechanism of the M2 proton channel of influenza A virus, Nature 451 (2008) 591–596.
[110] F.H. Hu, W.B. Luo, M. Hong, Mechanisms of proton conduction and gating in influenza M2 proton channels from solid-state NMR, Science 330 (2010) 505–508.
[111] M. Sharma, M.G. Yi, H. Dong, H.J. Qin, E. Peterson, D.D. Busath, H.X. Zhou, T.A. Cross, Insight into the mechanism of the influenza a proton channel from a structure in a lipid bilayer, Science 330 (2010) 509–512.
[112] G. Fiorin, V. Carnevale, W.F. DeGrado, The flu's proton escort, Science 330 (2010) 456–458.